Inward Propagating Chemical Waves in a Single-Phase Reaction-Diffusion System

Xin Shao,[1] Yabi Wu,[1] Jinzhong Zhang,[1] Hongli Wang,[1,2,3] and Qi Ouyang[1,2,3,*]

[1]*State Key Laboratory for Mesoscopic Physics, Department of Physics, Peking University, Beijing 100871, China*
[2]*The Beijing–Hong Kong–Singapore Joint Center for Nonlinear and Complex Systems (Peking University), Beijing, 100871, China*
[3]*Center for Theoretical Biology, Peking University, Beijing 100871, China*

(Received 25 September 2007; published 15 May 2008)

We report our experimental and theoretical studies of inwardly propagating chemical waves (antiwaves) in a single-phase reaction-diffusion (RD) system. The experiment was conducted in an open spatial reactor using chlorite-iodide-malonic acid reaction. When the system was set to near Hopf bifurcation point, antiwaves appeared spontaneously, as predicted using both the reaction-diffusion (RD) equation and the complex Ginzburg-Landau equation (CGLE). Antiwaves change to ordinary waves when the system was moved away from the Hopf onset, which still agreed with RD simulations but could not be predicted by CGLE. We thus witnessed a new type of antiwave—wave exchange. Our analysis showed that this exchange occurred when the CGLE broke down as the system was far from the Hopf onset.

DOI: 10.1103/PhysRevLett.100.198304 PACS numbers: 82.40.Ck, 47.20.Ky, 47.54.−r, 89.75.Kd

Recently, a new type of traveling waves, the inwardly rotating spirals (antispirals) and the inwardly propagating concentric waves (antitargets) were experimentally observed by Vanag *et al.* in the Belousov-Zhabotinsky (BZ) reaction that dispersed in water droplets of a water-in-oil aerosol OT (AOT) microemulsion (BZ-AOT system) [1–3]. This discovery raised great interests in the field of nonlinear dynamics. A series of theoretical studies have been carried out and the mechanism of antiwaves behavior has been explained using CGLE and the RD models [4–7]. While Vanag's experimental observations were successfully simulated using a model that describes the water-in-oil microemulsion system [2,3], theoretical studies suggest that antiwaves should exist in a simpler RD system, provided that the system is near the Hopf bifurcation [5–7]. However, so far no such observation has been reported in experiments. The purpose of this study is to identify antiwaves in a single-phase system, to study their behaviors, and to compare the experimental result with the theoretical predictions.

The chlorite-iodide-malonic acid (CIMA) reaction is one of the model systems in the investigation of pattern formations in RD media [8–11]. Two special features make this reaction suitable for the study. First, there exists a mathematical model that can faithfully describe the reaction dynamics [11–13]. Second, it is relatively easy to put the system near the Hopf bifurcation. Because of these two features, we selected CIMA reaction as our reaction system to investigate antiwaves. With the guide of the theoretical analysis, we purposely conducted our experiments near the onset of Hopf bifurcation. Both antitargets and antispirals were observed in the experiments. But we found that in most cases antitargets dominate the system because they had a larger oscillation period; it suppressed antispirals with smaller periods. We also observed ordinary spirals instead of targets when the system was away from the onset of Hopf bifurcation. The exchange of antiwaves to ordinary waves were different from the previous theoretical results predicted using CGLE.

Our experiments were conducted in a spatially open reactor as described in previous studies [9,10]. The reaction medium was a transparent disk of 2% agarose gel, 2 mm in thickness and 25 mm in diameter. A well-defined concentration of poly(vinyl alcohol) (PVA) was preloaded in the gel. Here, PVA acts both as a color indicator of tri-iodide ions in the reaction system and as an agent to influence the effective diffusivity of tri-iodide. In previous works [9,10], a high concentration of color indicators was used in the CIMA reaction to study Turing patterns. Here, we decreased its concentration so that Hopf bifurcation could take place. The agarose gel was sandwiched between two porous glass disks, which prevent PVA in the gel from flowing out, keeping the concentration of PVA in the reaction medium constant. The opposite two sides of porous glass disks were, respectively, in contact with two reactant reservoirs (I and II), where the reactants were continuously refreshed by highly precise chemical pumps and kept homogeneous by magnetically stirring. The whole system was surrounded with a thermostat; its temperature was kept at $8.0 \pm 0.5\,^{\circ}\mathrm{C}$. Images of traveling waves were registered by a CCD camera. The data were recorded in a computer via a frame grabber.

We chose the feeding concentration of malonic acid in reservoir I ($[MA]^{\mathrm{I}}$) as the control parameter. The concentrations of other reactants were kept fixed. The reaction condition was chosen so that the CIMA reaction was close to a supercritical Hopf bifurcation. The bifurcation takes place when $[MA]^{\mathrm{I}}$ is increased to across a threshold ($[MA]_c$) (value is extrapolated from the measurements of wave amplitude), so that $[MA]^{\mathrm{I}} - [MA]_c$ measures the distance from the onset. Under each condition, we waited enough time (two hours) before taking a record, so that the system could relax to its asymptotic state.

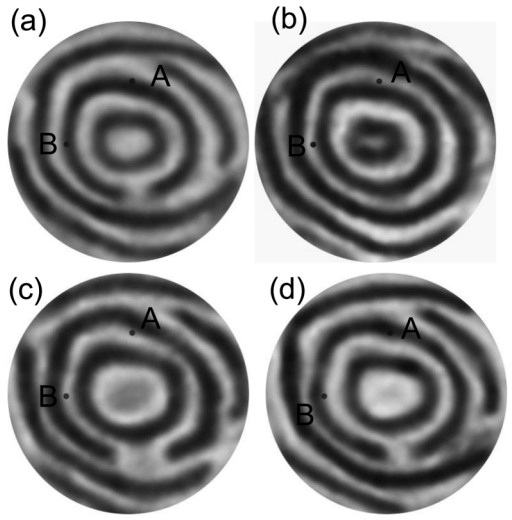

FIG. 1. Experimental observations of antitarget waves in the CIMA reaction. A and B are reference points. Pictures are recorded in different time within one period (a) $t = 0$, (b) $t = T/5$, (c) $t = 2T/5$, (d) $t = 3T/5$. The concentrations of the reactants are $[\mathrm{PVA}] = 5$ g/L, $[\mathrm{KI}]^{\mathrm{I,II}} = 3$ mM, $[\mathrm{Na_2SO_4}]^{\mathrm{I,II}} = 4.5$ mM, $[\mathrm{H_2SO_4}]^{I} = 20$ mM, $[\mathrm{NaClO_2}]^{\mathrm{II}} = 22$mM, $[\mathrm{NaOH}]^{\mathrm{II}} = 1$ mM, $[MA]^{\mathrm{I}} = 8$ mM. The field of view is 7.5 mm in diameter.

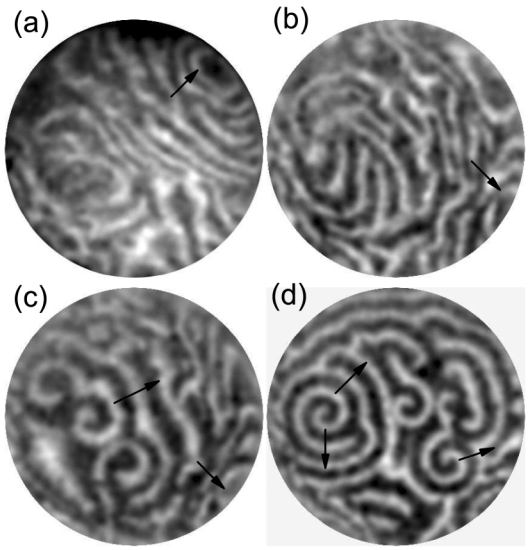

FIG. 2. Experimental observations of exchange of waves' behavior as the distance to the Hopf onset increases. $[MA]^{\mathrm{I}}$ in (a) 6 mM; (b) 8 mM; (c) 9 mM, (d) 12 mM. The concentrations of other reactants are kept fixed: $[\mathrm{PVA}] = 6$ g/L, $[\mathrm{KI}]^{\mathrm{I,II}} = 3.6\ mM$, $[\mathrm{Na_2SO_4}]^{\mathrm{I,II}} = 4.5$ mM, $[\mathrm{H_2SO_4}]^{\mathrm{I}} = 20$ mM, $[\mathrm{NaClO_2}]^{\mathrm{II}} = 22$ mM, $[\mathrm{NaOH}]^{\mathrm{II}} = 1$ mM.

When the control parameter was set to beyond but near the critical value, antitarget waves and antispiral waves spontaneously appeared in the reaction medium. Usually the period of antitargets were larger than that of antispirals, asymptotically an antitarget dominated the whole system. A sequence of snapshots in Fig. 1 (see also supplementary video [14]) shows a typical example of an antitarget. One observes that chemical waves emerge at the periphery, propagate inwardly, collide, and disappear at a center. These kinds of waves are qualitatively different from the ordinary target waves. The wavelength of the antitarget was measured to be 0.94 mm, the period was 50 s, and the wave speed was 0.019 mm/s.

In order to build a phase diagram of the system, we systematically changed the control parameter to adjust the distance to the onset of Hopf bifurcation, which was measured to be $[MA]_c = 5.0$ mM. At $[MA]^{\mathrm{I}} = 6.0$ mM, an antitarget was observed at upright corner of the system, as the arrow pointed in Fig. 2(a). But disordered plane waves appeared far away from the target center (it is hard to tell these plane waves propagated outwardly or inwardly). At $[MA]^{\mathrm{I}} = 8.0$ mM, the antitarget began to be suppressed by plane waves, as shown in Fig. 2(b). In this case, the center of the antitarget (pointed by an arrow) was almost pushed out of the reaction medium by plane waves. The plane waves changed to outwardly rotating spirals when the $[MA]^{\mathrm{I}}$ was further increased, as shown in Fig. 2(c). At the same time, antitarget disappeared at the boundary. When $[MA]^{\mathrm{I}}$ became 12.0 mM, the system was full of outwardly rotating spirals [Fig. 2(d)].

The phase diagram was recorded in Fig. 3(a), which also included the period of different waves. The diagram can be split into three different regimes, an antitarget regime (AT), an antitarget–ordinary spiral transition regime (AT–OS), and ordinary spiral regime (OS). Although previous analysis using CGLE predicted that wave–antiwave transition takes place when the wave number k goes to zero [4–7], we did not observe such transition in experiments. Instead we saw [Fig. 2(c)] ordinary spirals gradually push antitargets out of the system.

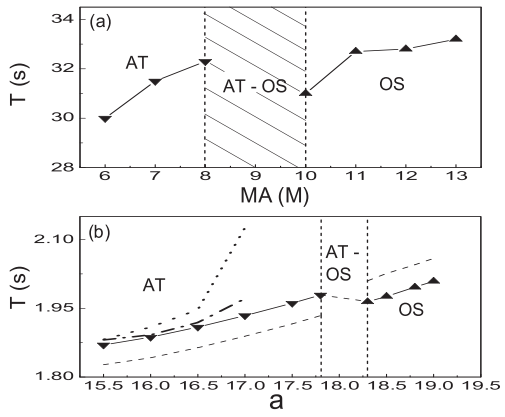

FIG. 3. (a) Measured periods of the antitargets (▼) and the normal spirals (▲) in CIMA reaction with different concentrations of MA. (b) Measured periods of the antitargets (▼) and the spirals (▲) in the CIMA RD model as a function of a; the solid lines represent the winning pattern in the competition between target and spiral in the RD medium, and the dashed line represents the loser one. The dotted line and the dash-dotted line give, respectively, the behavior of the targets and the spirals predicted by CGLE. Here AT represents antitarget, AT-OS represents antitarget—ordinary spiral transition, and OS represents ordinary spiral.

To understand the dynamics underlying the phenomena presented above, we conducted computer simulations and theoretical analysis. The CIMA reaction mechanism in a homogeneous RD medium can be described by the Lengel-Epstein model [11–13]. The no-dimensional form of the equations are as follows:

$$\begin{aligned} \partial x/\partial t &= a - x - 4xy/(1+x^2) + D_x\nabla_r^2 x \\ \partial y/\partial t &= b[x - xy/(1+x^2)] + D_y\nabla_r^2 y, \end{aligned} \tag{1}$$

where x and y represent, respectively, the no-dimensional concentration of I^- and ClO_2^-; a and b are parameters determined by the control parameters in the experiment. There is a unique uniform steady state solution in Eq. (1) given by $(x_0, y_0) = (a/5, 1 + a^2/25)$. The linear stability analysis of the fixed point (x_0, y_0) showed that the steady state becomes unstable and the system undergoes a Hopf bifurcation if $b < b_c = 3a/5 - 25/a$. This transition induces periodic oscillations of the concentrations in the CIMA reaction, with an oscillation amplitude $|A|$ and an intrinsic frequency $\omega_c = \sqrt{\frac{5(3x_0^2-5)}{1+x_0^2}}$ $(a > 5\sqrt{5/3})$ at onset.

To conduct nonlinear analysis and get the corresponding CGLE from the RD model, solutions (x, y) in Eq. (1) were decomposed as [15,16]:

$$\begin{pmatrix} x \\ y \end{pmatrix} = \begin{pmatrix} x_0 \\ y_0 \end{pmatrix} + \begin{pmatrix} x_1 \\ y_1 \end{pmatrix} A(\mathbf{r}, t)e^{i\omega_c t} + c.c. \tag{2}$$

Using the reductive perturbation method and after an intensive analytical study, we derived the corresponding CGLE of Eq. (1):

$$\frac{\partial W}{\partial t'} = W - (1 + i\alpha)W \mid W \mid^2 + (1 + i\beta)\nabla_{r'}^2 W, \tag{3}$$

where

$$\begin{aligned} &\alpha = \alpha_1/\alpha_2, \qquad \alpha_1 = \frac{2x_0^4 - 27x_0^2 - 5}{2x_0^2(1+x_0^2)^2}, \\ &\alpha_2 = \frac{26x_0^6 - 119x_0^4 + 100x_0^2 - 75}{30x_0^2(3x_0^2-5)(1+x_0^2)^2}\omega_c, \qquad \beta = \beta_1/\beta_2, \\ &\beta_1 = \frac{D_x + D_y}{2}, \qquad \beta_2 = \frac{D_x - D_y}{10}\omega_c, \\ &A = \sqrt{\frac{-a_1(b-b_c)}{\alpha_1}}\exp\left(i\frac{a_2}{a_1}t'\right)W, \\ &r = \sqrt{\frac{\beta_1}{a_1(b-b_c)}}r', \qquad t = \frac{1}{a_1(b-b_c)}t', \\ &a_1 = \frac{-x_0}{2(1+x_0^2)}, \qquad a_2 = \frac{x_0}{2(3x_0^2-5)}. \end{aligned} \tag{4}$$

The CGLE has a traveling wave solution $W(\mathbf{r}', t') = F(r')e^{i(k_{\mathrm{CGLE}}r' - \omega_{\mathrm{CGLE}}t')}$ with a selected wave number k_{CGLE} and a frequency $\omega_{\mathrm{CGLE}} = \alpha + (\beta - \alpha)k_{\mathrm{CGLE}}^2$. Translating this analytical result back to the RD system, we deduced that the wave number of the traveling wave in CIMA reaction should be

$$k_{\mathrm{CIMA}} = \sqrt{\frac{a_1(b-b_c)}{\beta_1}}k_{\mathrm{CGLE}} \tag{5}$$

and the frequency ω_{CIMA} should be:

$$\omega_{\mathrm{CIMA}} = (\omega_{\mathrm{CGLE}} - a_2/a_1)a_1(b - b_c) - \omega_c \tag{6}$$

Thus the group velocity of waves in the RD reaction is $v_{\mathrm{gr}} = \frac{\partial\omega_{\mathrm{CIMA}}}{\partial k_{\mathrm{CIMA}}} = 2\sqrt{\frac{2a_1(b-b_c)}{D_x+D_y}}(\beta - \alpha)k_{\mathrm{CGLE}}$. Note that since the wave number k_{CGLE} takes the same sign as $\beta - \alpha$ [5,17], the group velocity is positive. Then the phase waves move outwardly (inwardly) for positive (negative) phase velocity. The phase velocity is calculated to be $v_{\mathrm{ph}} \approx -\omega_c\sqrt{\frac{D_x+D_y}{2a_1(b-b_c)}}/k_{\mathrm{CGLE}}$, so that v_{ph} is negative when k_{CGLE} is negative, i.e., when $\alpha < \beta$. If we set $b = 7.6$, $D_x = 0.07$, $D_y = 0.075$ in Eq. (1) as Ref. [11], this condition in the Lengel-Epstein model means antiwaves appear when $a > 9.9$. Since the onset of Hopf bifurcation is $a_{\mathrm{Hopf}} \approx 15.4$ under the given condition, the pattern observed in the RD medium should be antiwaves. To test this prediction, we integrated Eq. (1) with $a = 15.5$, which corresponds $\alpha = -1.524$ and $\beta = -0.023$ in Eq. (3). The simulation result [Figs. 4(a) and 4(b)] indeed shows target and spiral waves propagating inwardly, as the arrows point.

In the following, our simulation and analysis were focused on the pattern competition in order to explain three different regimes observed in the experiment. The RD model of Eq. (1) were used in the simulation, which started when the system is near the Hopf onset. The initial condition is an antispiral. Then we introduce an inhomogeneity in the medium by choosing a small area (3×3 grids) away from the spiral tip and keeping the values of $x = 0$ and $y = 0$ in the region. This small area plays as a pacemaker of target waves in simulations. Typical examples of simulation results are illustrated in Fig. 4. The period of the spirals and the targets as a function of the control parameters a are plotted in Fig. 3(b). At a low value of a, the system was near the onset of Hopf bifurcation. As pre-

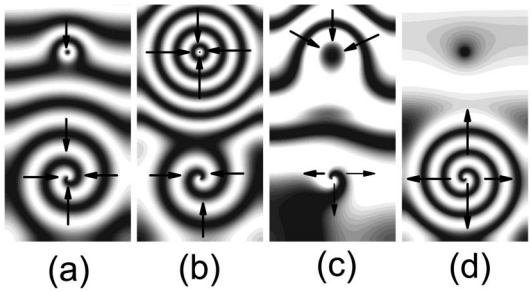

FIG. 4. Simulation results of dimensionless Lengyel-Epstein model for $b = 7.6$, $D_x = 0.07$, $D_y = 0.075$. a: (a) 15.5, t_1; (b) 15.5, t_2 $(t_2 > t_1)$; (c) 18.0; (d) 18.5. The system moves away from Hopf onset as a increases. Equation (1) is integrated using the alternating-direction implicit method (ADI) with no-flux boundary conditions. The time and spatial steps are 0.01 and 2.0, respectively.

dicted by the CGLE, both antitarget and antispiral could be seen in the medium separately; the period of antitargets was larger than that of antispirals [Fig. 3(b)]. However, when they coexist in the same medium [Fig. 4(a)], the antitarget will gradually suppressed the antispiral, which can be seen from Fig. 4(b). The reason is that, given the same wavelength, an inwardly propagating wave with a longer period will spend a longer time to collide in the wave center, making its wave number larger. Eventually only the antitarget could be observed in this area. This is consistent with the experimental observation.

When we increased the value of a, the system would go far away from the Hopf onset. In this process we obtained antitarget—ordinary spiral exchanges. The transition from the antitarget to ordinary spiral is very slow; as a result, we had a region of overlap ($17.8 < a < 18.3$) where both antitarget and ordinary spiral could be seen in the medium. Taking $a = 18.0$ as an example, both antitarget and ordinary spiral can be observed in the simulation result [Fig. 4(c)]. The mechanism of this kind of transition between antitargets and spirals is still not clear now, which also exists in the experiments. Notice that according to the CGLE prediction, all patterns observed under the conditions given by Fig. 4 should be antiwaves, and the antiwave–wave exchange should occur only through $k \to 0$ [5,6]. Here in the RD simulation, we witnessed a different type of transition where antitarget is gradually pushed out by spiral, which could not be explained by CGLE. As the control parameter a was further increased so that the system was further away from the Hopf onset, we observed only a normal spiral, as shown in Fig. 4(d). For normal waves, a larger period provides a disadvantage in pattern competition (just opposite to antiwaves), spiral waves will eventually suppress target pattern in the RD medium [seen in Fig. 3(b)].

We notice that in the regime of antiwave—wave exchange there exists a disagreement between experimental observation and simulation. In the experiments, the exchange accompanied by the appearance of disordered plane wave (Fig. 2), while in the simulations no such phenomenon was observed. The reason of the appearance of disordered waves is not yet clear; we suspect the slight inhomogeneity of the experimental medium is one of the major causes.

At last, we checked the validity of the CGLE when the RD system went far away from the onset of Hopf bifurcation. To do this, we monitored the period of targets and spirals measured in the RD system and the corresponding CGLE in simulations. The value of α and β in the CGLE were deducted from Eq. (4) and the dimensionless period in the CGLE was translated using Eq. (6). As shown in Fig. 3(b), when the control parameter a was near the Hopf bifurcation point, the periods predicted by the CGLE is close to the real periods measured in the RD system. On the contrary, when the value of a increased so that the RD system is away from the Hopf onset, the difference in the periods diverged. This study demonstrates that the CGLE is a good approximation of the RD system only when the RD system is close to the Hopf onset. When the RD system goes far away from the onset, the CGLE cannot be used to forecast patterns behavior in the RD system any more.

In conclusion, this study presents a clear example of antiwaves in a simpler single-phase RD system. A new type of phase diagram was observed both in experiments and in RD simulations, which could not be predicted using the CGLE. The breakdown of CGLE in this case reminds us that one needs to be very careful in using CGLE to study a RD system, especially when the RD system is away from the onset of Hopf bifurcation. Finally, we notice that a new type of metamaterial so-called ''left hand'' media has been in the frontier research in the condensed matter physics. In this type of metamaterials electromagnetic waves behave like antiwaves [18]. The study of the antiwaves in nonlinear systems may provide some hint in this field of study.

This work is partially supported by the Chinese Natural Science Foundation, the Ministry of Science and Technology in China, and the National Fund for Fostering Talents of Basic Science (No. J0630311).

*To whom correspondence may be addressed.
qi@pku.edu.cn

[1] V. K. Vanag and I. R. Epstein, Science **294**, 835 (2001).
[2] V. K. Vanag and I. R. Epstein, Phys. Rev. Lett. **87**, 228301 (2001).
[3] V. K. Vanag and I. R. Epstein, Phys. Rev. Lett. **88**, 088303 (2002).
[4] H. L. Wang and Q. Ouyang, Chin. Phys. Lett. **21**, 1437 (2004).
[5] L. Brusch, E. M. Nicola, and M. Bär, Phys. Rev. Lett. **92**, 089801 (2004).
[6] E. M. Nicola, L. Brusch, and M. Bär, J. Phys. Chem. B **108**, 14 733 (2004).
[7] C. Wang, C. X. Zhang, and Q. Ouyang, Phys. Rev. E **74**, 036208 (2006).
[8] V. Castets, E. Dulos, J. Boissonade, and P. DeKepper, Phys. Rev. Lett. **64**, 2953 (1990).
[9] Q. Ouyang and H. L. Swinney, Nature (London) **352**, 610 (1991).
[10] Q. Ouyang and H. L. Swinney, Chaos **411**, 1 (1991).
[11] I. Lengyel and I. R. Epstein, Science **251**, 650 (1991).
[12] I. Lengyel, G. Rabai, and I. R. Epstein, J. Am. Chem. Soc. **112**, 9104 (1990).
[13] I. Lengyel, S. Kadar, and I. R. Epstein, Phys. Rev. Lett. **69**, 2729 (1992).
[14] See EPAPS Document No. E-PRLTAO-100-060820 for a supplementary video. For more information on EPAPS, see http://www.aip.org/pubservs/epaps.html.
[15] Y. Kuramoto, *Chemical Oscillations, Waves, and Turbulence* (Springer-Verlag, Berlin, 1984).
[16] G. Nicolis, *Introduction to Nonlinear Science* (Cambridge University Press, Cambridge, U.K., 1993).
[17] P. S. Hagan, SIAM J. Appl. Math. **42**, 762 (1982).
[18] D. R. Smith, W. J. Padilla, D. C. Vier, S. C. Nemat-Nasser, and S. Schultz, Phys. Rev. Lett. **84**, 4184 (2000).